

Supplemental Materials

Detailed Materials & Methods

Mice & in vivo procedures

The *Hprt-lsl-IRFP* allele was previously described [33]. All mice were maintained on a mixed FVBN/C57Bl6 background, housed on a 12-hour light/dark, cycle and fed and watered ad libitum. Recombinant adenoviruses expressing CRE (Ad-CMV-CRE & Ad5mSPC-CRE) were purchased from the University of Iowa gene therapy facility. For adeno-CRE installation, young adult (8- to 10-week-old) mice were sedated with a mixture of medetomidine and ketamine, injected IP. For most experiments, 1×10^7 pfu adeno-CRE were administered intranasally using the calcium phosphate precipitation method, as described previously [35]. For lower tumor burden, 5×10^4 - 3×10^5 pfu were administered. Neratinib (Medchem Express) was administered by twice-daily gavage of 40 mg/kg for up to 4 weeks, or a single daily IP injection of 80 mg/kg for short-term (3-7 days) experiments. Erlotinib (Apex-Bio) was given by twice daily gavage of (50mg/kg). For gavage, 0.5% methylcellulose and 0.4% Tween-80 in H₂O was used as vehicle; peanut oil was used for IP. Trametinib (LC Labs) was administered by single daily IP injection at 1 mg/kg. Live imaging of iRFP-positive tumor-bearing mice was performed using a PEARL imaging system (Licor). All mice were sacrificed humanely by CO₂ inhalation followed by cervical dislocation.

Immunohistochemistry and Tissue Analysis

Mouse tissues were perfusion-fixed in zinc formalin overnight. 4- μ m paraffin sections were deparaffinized and rehydrated: 3 x 5 minutes xylene, 2 minutes each in 2x100%; 2x95%; 2x70%; 1x50% ethanol; dH₂O. Peroxidase blocking was performed for 10 min in 3% H₂O₂ diluted in H₂O, followed by antigen retrieval in 10 mM citrate buffer, pH 6, 10 min near boiling by microwave heating at low power. Non-specific antibody binding was blocked with up to 3% BSA or up to 5%

normal goat serum for 1 hour at room temperature (RT) or overnight at 4°C. Primary antibody incubation was performed overnight at 4°C or 2 hours at 37°C. Secondary biotinylated antibody was incubated for 1 hour at room temperature, and the stain was developed with stable DAB (Invitrogen) followed by counterstaining with Gil 1 hematoxylin (Sigma MH216) and Scotts tap water substitute. The following antibodies were used at the indicated dilution: p-ERK (P44/42 MAPK phospho-Thr202/Tyr204), Cell Signaling CS4370, 1:500; Ki67 (Sp6), Fisher Scientific RM9106S 1:200; SP-C, Millipore AB3786, 1:1000; CC10, Millipore 07-623, 1:1000; TUNEL ApopTag kit, Millipore S7100; Vectorlabs VECTASTAIN ABC kit; anti-rabbit IgG, PK-4001 ECL; anti-rat, GE Healthcare NA935. Ki67 and TUNEL labeling was scored manually on 5 tumors from each mouse, and graphs show mean values \pm SE from the indicated number of mice. Tumor burden was determined using Halo software (Indica Labs) as the % area of lung tissue occupied by tumors, measured on hematoxylin & eosin (H&E) stained sections at 100 μ m intervals through the entire tissue block, from each of the indicated numbers of mice. Histological classification of tumors as adenocarcinoma and identification of p-ERK^{High}- and *Areg*-expressing cells as epithelial was performed independently by 2 clinical pathologists.

In Situ Hybridization

5 μ m tissue sections on Superfrost Ultra plus slides were incubated at 60°C for 2 hours. The sections were then placed onto a Leica Bond Rx autostainer and stained overnight with the probe of interest using a RNAscope 2.5 LS reagent brown kit (Leica Systems 322100). The staining protocol was fully automated and included the following steps: Dewaxing using Leica Bond Dewaxn (AR9222) solution; washing with Leica Bond Wash solution (AR9590); Denaturing (antigen retrieval) using Leica Bond Epitope Retrieval one solution (AR9661) at 98°C for 15 followed by rinsing in Bond Wash. Leica Enzyme III (AR9551) was applied for 15 minutes followed by rinsing with Bond Wash. *Areg*- or *Ereg*-specific probes were incubated for 2 hours at 40°C, followed by

rinsing in Bond Wash. Sections were subject to 6 rounds of signal amplification using the 2.5 LS reagent brown kit according to manufacturer's instructions (Leica Systems). After application of probe 6, sections were rinsed and DAB solution from the 2.5 LS reagent kit applied to the sections for 20 minutes at room temperature. Sections were then rinsed in water with haematoxylin and bluing agent from the 2.5 LS kit applied to counterstain nuclei. Following standard dehydration in graded alcohols, sections were mounted with a glass coverslip on a Leica CV5030 coverslipper using CellPath DPX mounting medium (SEA-1300-00A).

Laser-Capture Microdissection & RNA-SEQ analysis

For micro-dissection, 10 μm FFPE sections were mounted on framed membrane slides (Leica). Adjacent sections were mounted on standard poly-L-lysine-coated glass slides and stained for p-ERK. Membrane slide-mounted tissue was de-paraffinized, rehydrated, and stained with ice-cold 1% cresyl violet. Selected tissue was micro-dissected using a Leica DM 6000B microscope, and total time for staining and micro-dissection was under 20 minutes per sample. P-ERK^{LOW} and p-ERK^{HIGH} tumor regions were harvested into separate tubes, and tissue from multiple sections was pooled for each of 4 mice. Harvested tissue was suspended in 30 μl PKD buffer (Qiagen, RNEasy FFPE kit) and flash-frozen for storage. Total tissue RNA was isolated using the RNEasy FFPE kit according to manufacturer's directions, and ribosomal RNA was depleted with Ribo-Zero (Epicentre). Synthesis of cDNA was performed using the SMARTER Stranded random primed RNA-SEQ kit (Takara/Clontech), resulting in cDNA libraries flanked by Illumina indexing primers. After library quantification (Quant-IT Pico green kit, Invitrogen), libraries were standardized to 10 nM, denatured, diluted to 10 pM, and analyzed by paired-end sequencing with an Illumina GA11X deep sequencer. The raw RNA-sequencing data files underwent quality checks using FastQC and FastQ-Screen software. RNA-sequencing reads were aligned to the GRCm38 [42] version of the mouse genome using Tophat2 version 2.0.10 [43] with Bowtie version 2.1.0 [44]. Relative expression was

determined and statistically analyzed by a combination of HTSeq and the R 3.0.2 environment, using packages from the Bioconductor data analysis suite and differential gene expression analysis based on the negative binomial distribution in the EdgeR package [45]. Pathway modulation analysis was performed with Metacore GeneGO (Thompson Reuters). For analysis of individual gene expression, data were normalized to *B2m* for each mouse, and fold change and false discovery rates were recalculated. RNA-SEQ analysis of human cell lines: Total RNA was isolated using the RNEasy Mini Kit (Qiagen) according to manufacturer's instructions, and DNA was depleted with the RNase-Free DNase Set (Qiagen). RNA integrity was checked using the RNA ScreenTape assay (Agilent Technologies), and cDNA was synthesized with the TruSeq Stranded mRNA Library Prep Kit (Illumina). After library quantification (D1000 ScreenTape, Agilent Technologies), libraries were standardized to 10 nM, denatured, diluted to 10 pM, and analyzed by paired-end sequencing using an Illumina NextSeq500 platform. RNA-Sequencing reads were aligned to the GRCh37 version of the human genome and differential expression determined with DESeq2 [46].

Figure S1

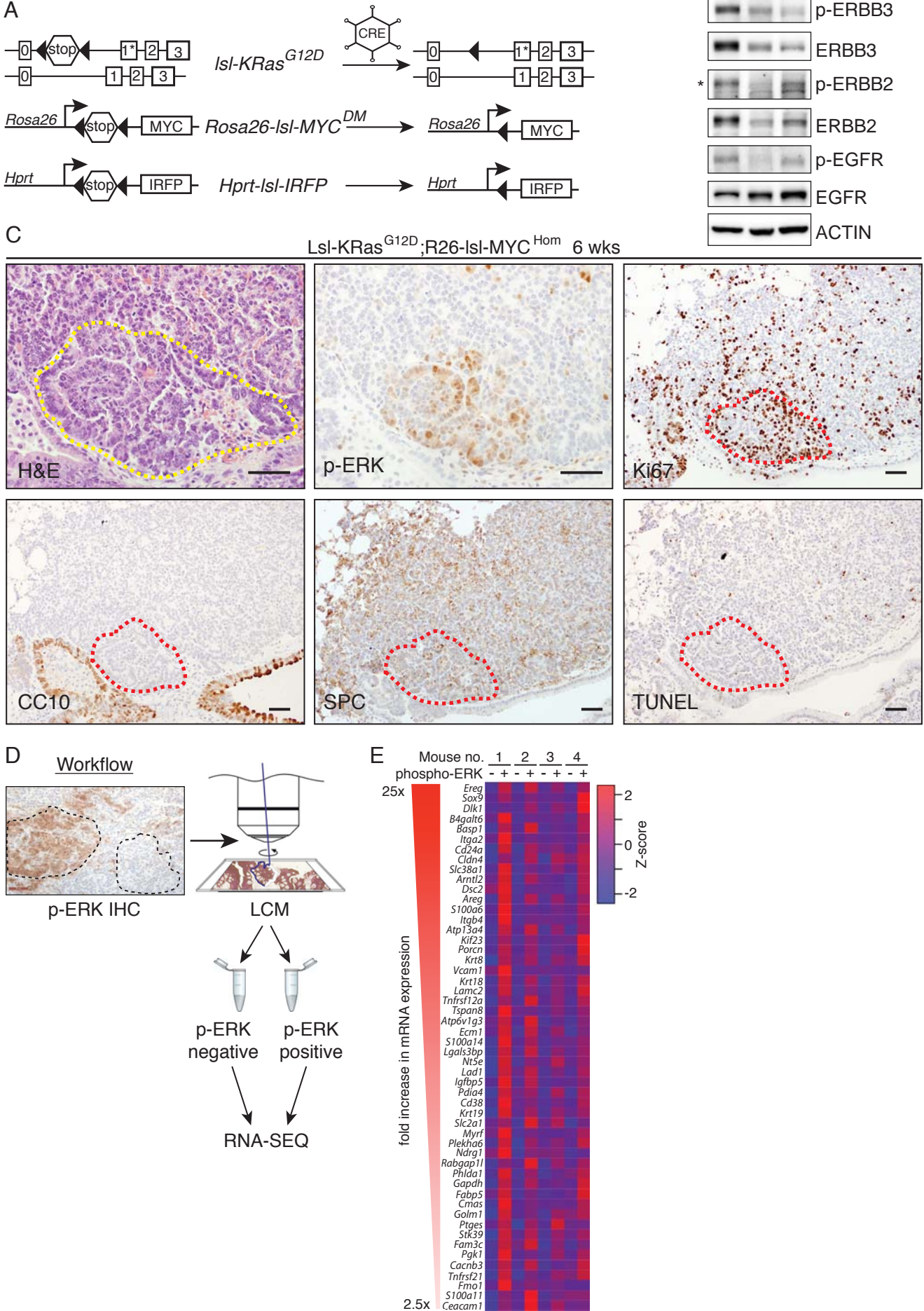


Figure S1: Characterization of KM lung tumors.

A) Schematic of allele activation: Adult (8- to 10-week-old) mice bearing the indicated conditional alleles were given recombinant adeno-CRE via intranasal instillation and monitored for the durations indicated in the text, or until symptomatic. **B)** Immunoblots of lysates from individual KM tumors induced with Ad5mSPC-CRE (lanes 1&2) and treated with neratinib (lane 2), compared with normal lung (lane 3). **C)** Serial sections from an *Isl-KRas^{G12D};R26-Isl-MYC^{Hom}* mouse lung harvested at 6 weeks post induction (PI) and stained with the indicated antibodies or TUNEL. Scale bars = 50 μ m. Images are representative of lungs from at least 5 mice analyzed for each stain. Outline demarcates the approximate p-ERK-positive tumor region. **D)** Workflow of laser-capture micro-dissection (LCM) of FFPE KM lung tumors. Serial sections were first stained for p-ERK expression to identify p-ERK^{High} and p-ERK^{Low} tumor regions. Cresyl violet-stained adjacent sections were then subject to LCM upon identification of the corresponding regions. Messenger RNA was purified from harvested material and analyzed by RNA-SEQ. **E)** Gene signature of progression from p-ERK^{Low} to p-ERK^{High} KM tumors triaged to only include genes either amplified or overexpressed in human LuAd data sets [2, 8, 9, 47]. Results from 4 mice shown.

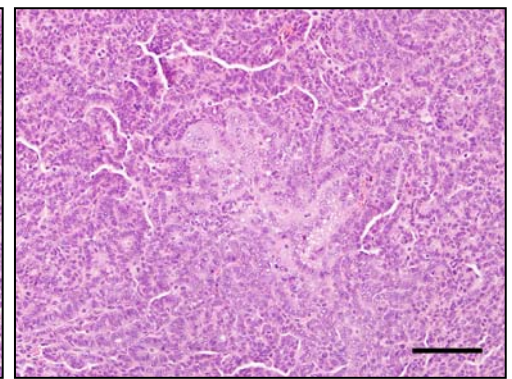
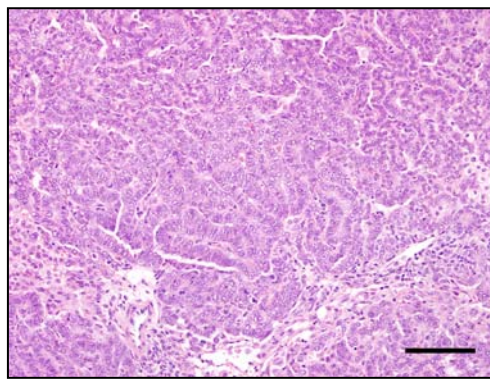
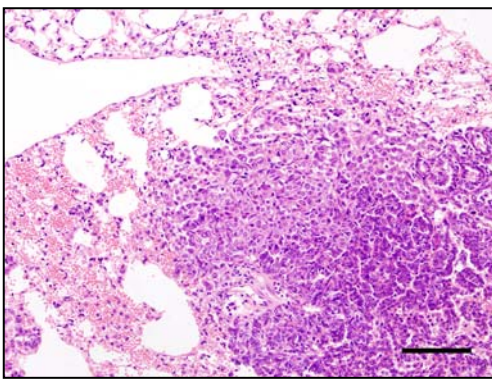
Figure S2

A

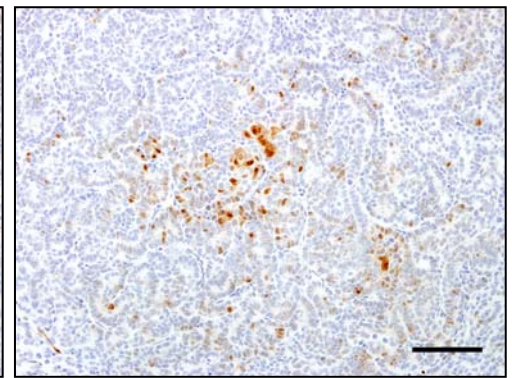
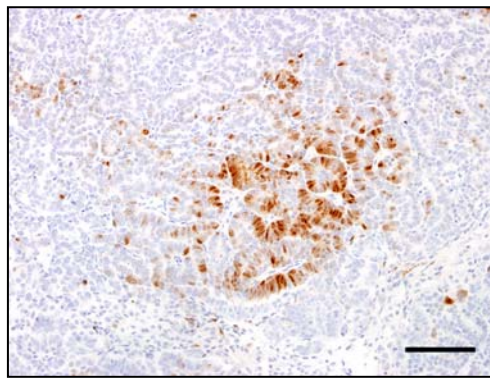
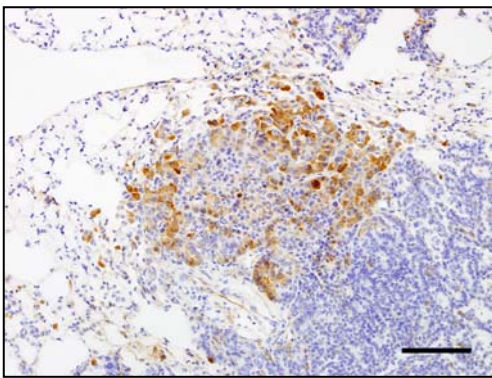
Ad-CMV-CRE

Ad-SPC-CRE

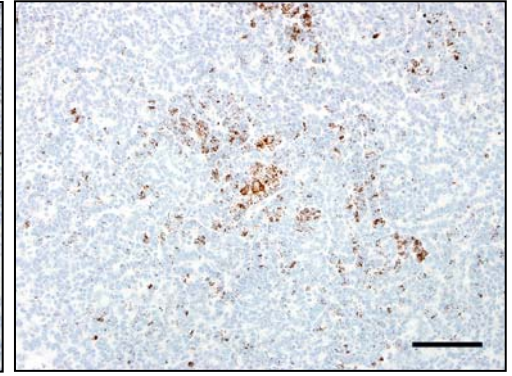
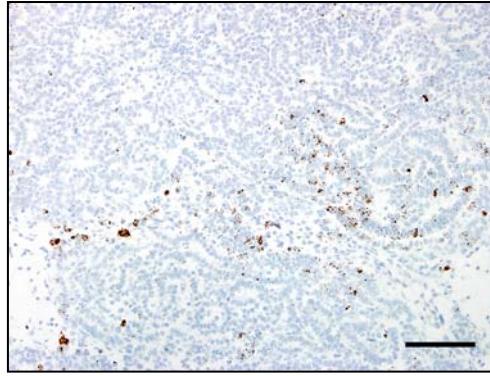
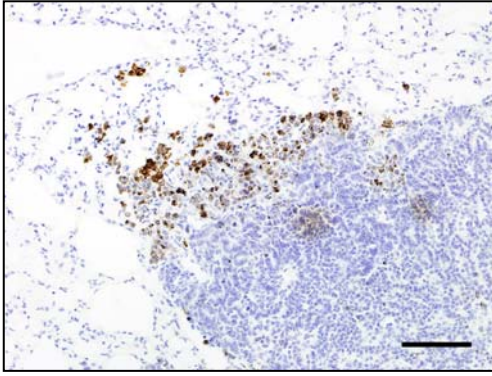
H&E



p-ERK



Areg



F4/80

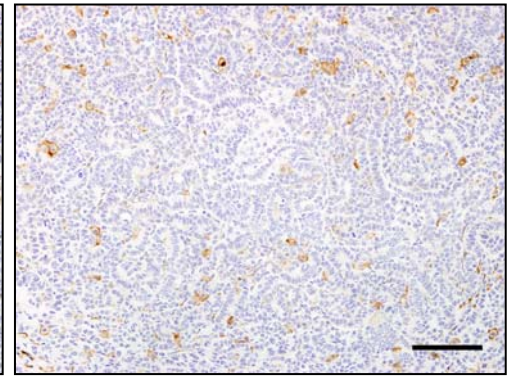
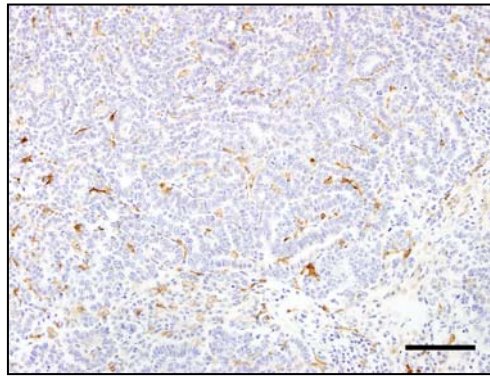
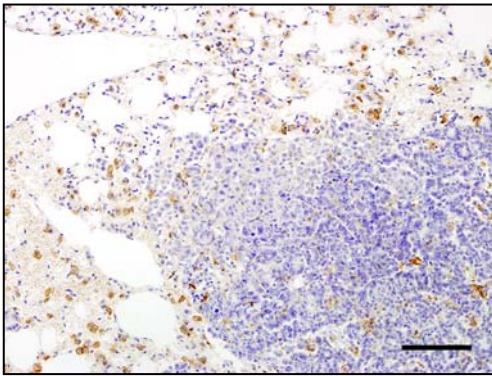


Figure S2

B

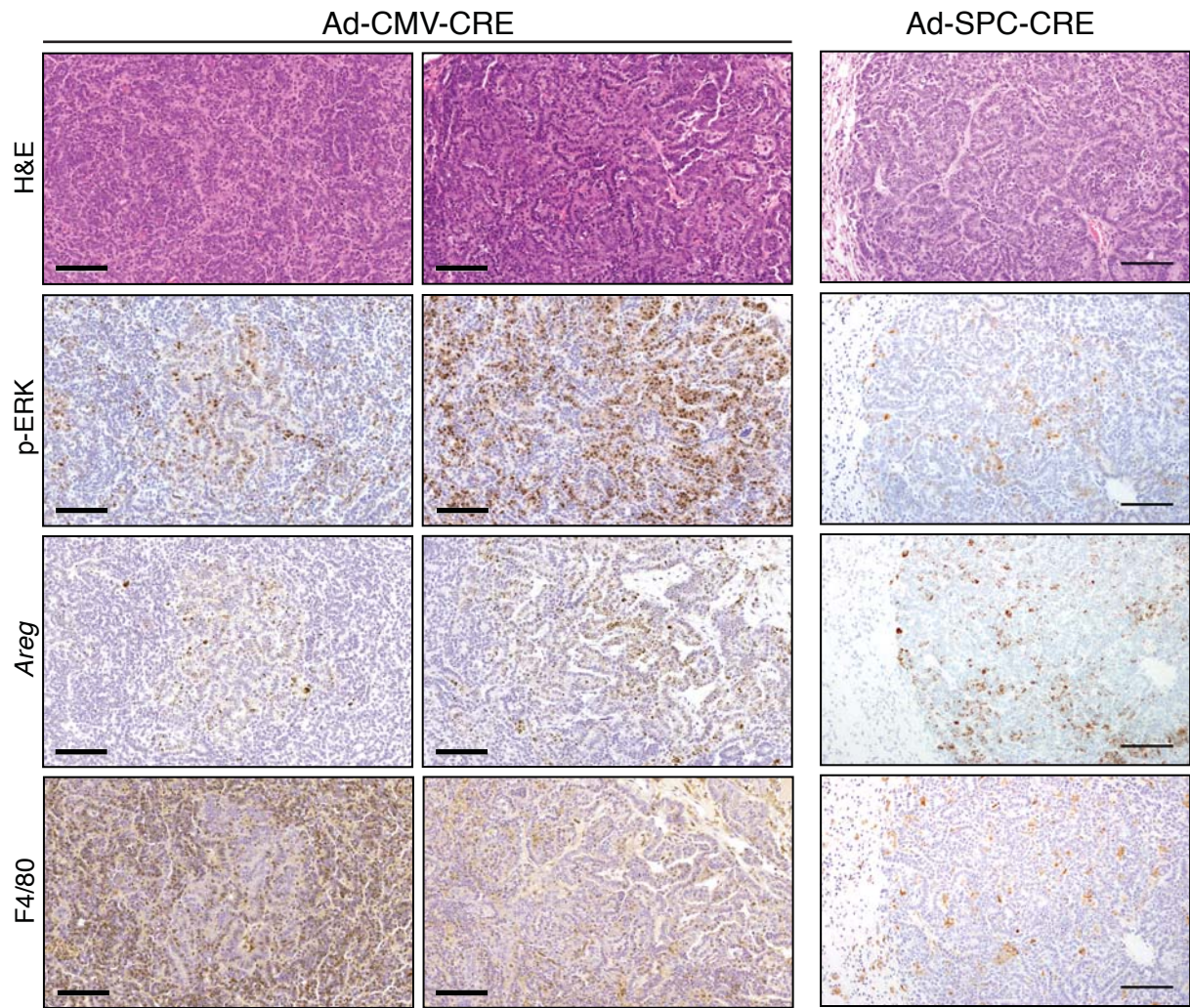


Figure S2

C

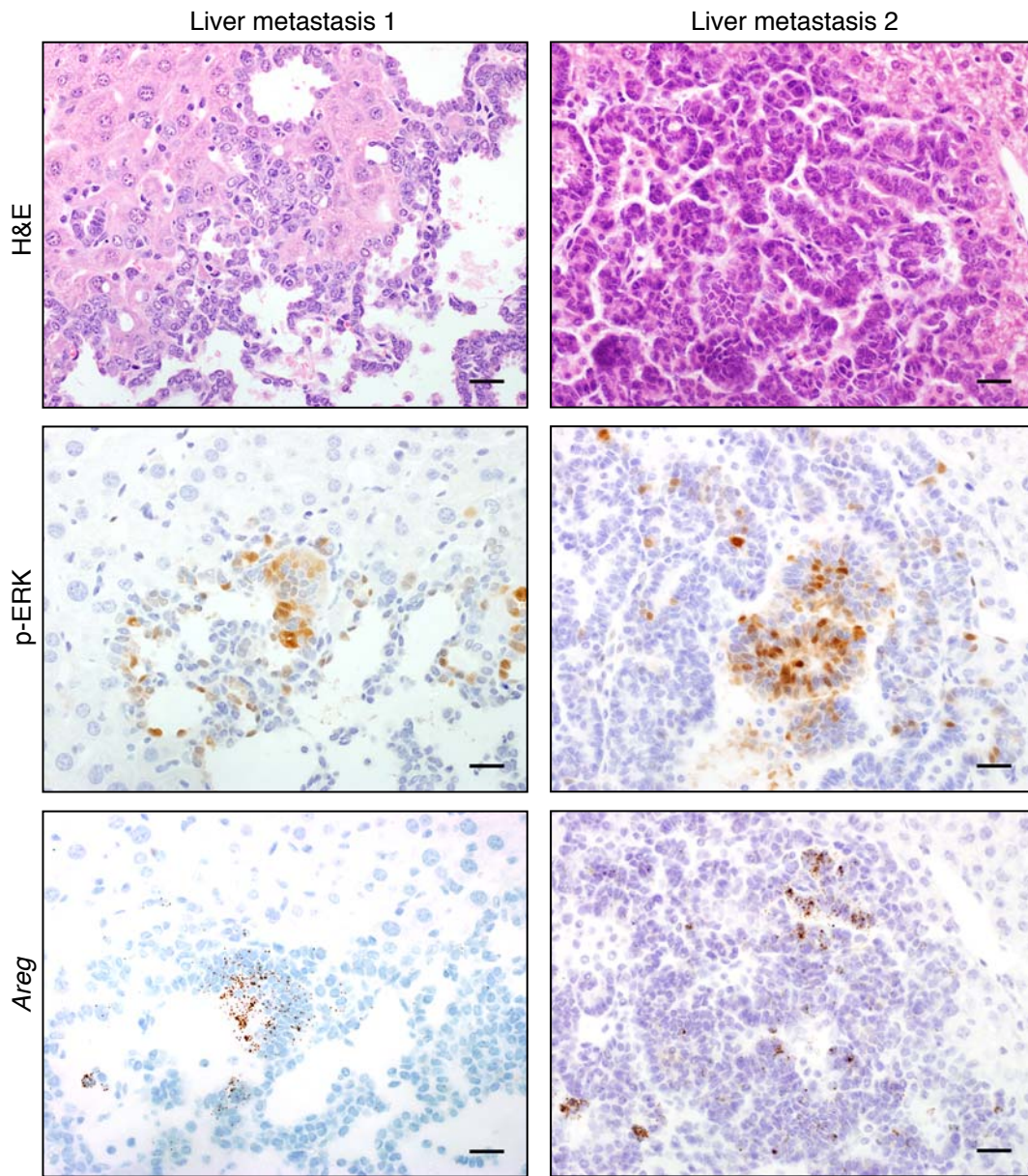


Figure S2: Comparison of KM phenotype induced by Ad-CMV-CRE & Ad-SPC-CRE

A) Serial sections show representative images of KM lungs induced by the indicated CRE-delivery vectors harvested and analyzed at 6 weeks post induction. H&E, IHC for p-ERK and F4/80 (macrophages), along with ISH for *Areg* mRNA are shown. Scale bars = 100 μ m. **B)** Additional examples of IHC and *Areg* ISH in primary lung tumors from Ad-CMV-CRE and Ad-SPC-CRE induced KM mice. Scale bars = 100 μ m. **C)** Additional examples of p-ERK IHC and *Areg* ISH in liver metastases from KM mice. Scale bars = 25 μ m.

Figure S3

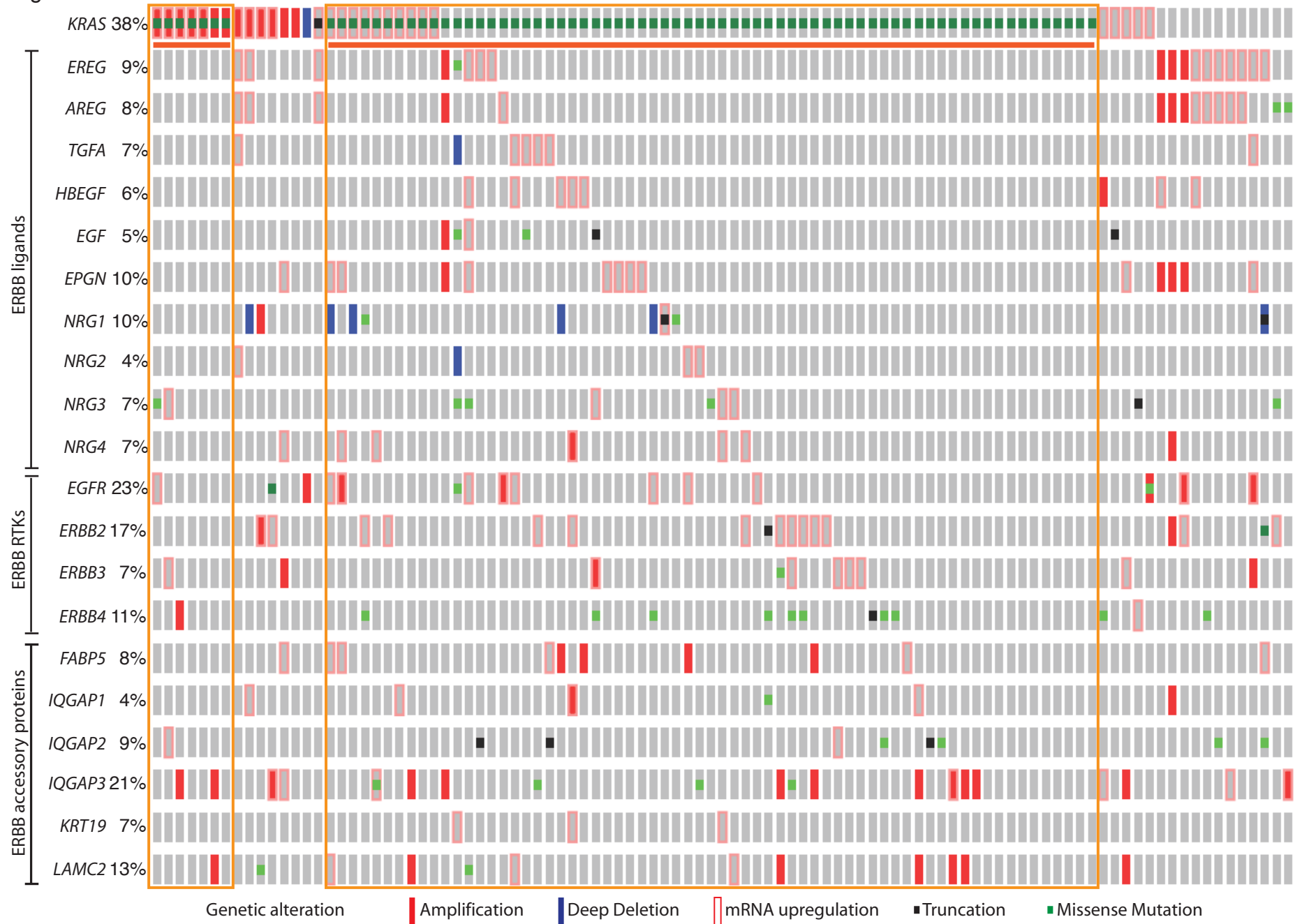


Figure S3: Genomic alterations and expression of ERBB network genes in human KRAS-mutant lung adenocarcinoma.

Each column represents an individual tumor. Genes are grouped as ERBB ligands, ERBB RTKs and ERBB accessory proteins. Percentages refer to the frequency of alteration across all lung adenocarcinomas. Orange bars (top) emphasize cases with KRAS mutations (n=74, of which 73 are codon 12 mutant), and orange boxes outline the ERBB network in the same cases. Green dots indicate codon alterations; black dots indicate truncation mutations; solid red bars denote gene amplifications; open red bars show increased mRNA expression; solid blue bars indicate deep deletions. Gray bars indicate no detected alteration. Data are derived from the published TCGA lung adenocarcinoma cohort as accessed via cBioportal (truncated from the right to focus on the KRAS-mutated patient subset).

Figure S4

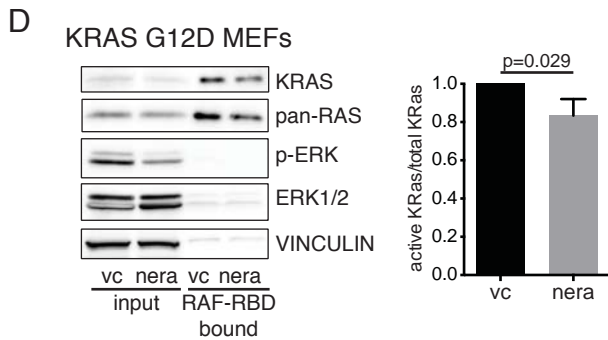
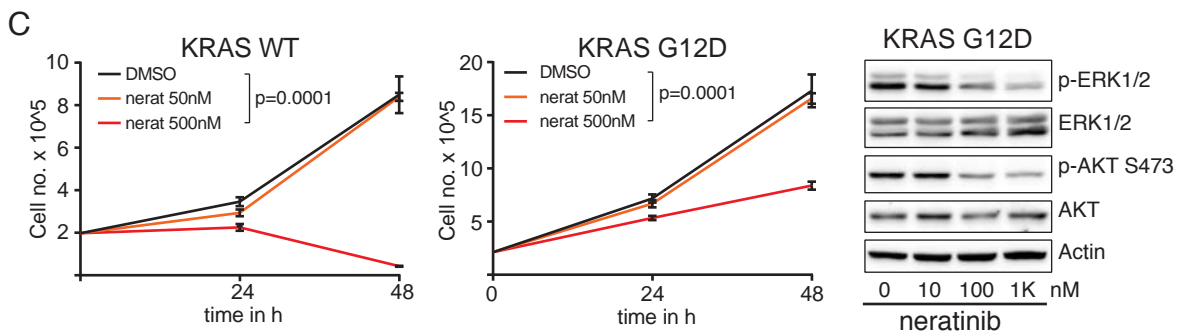
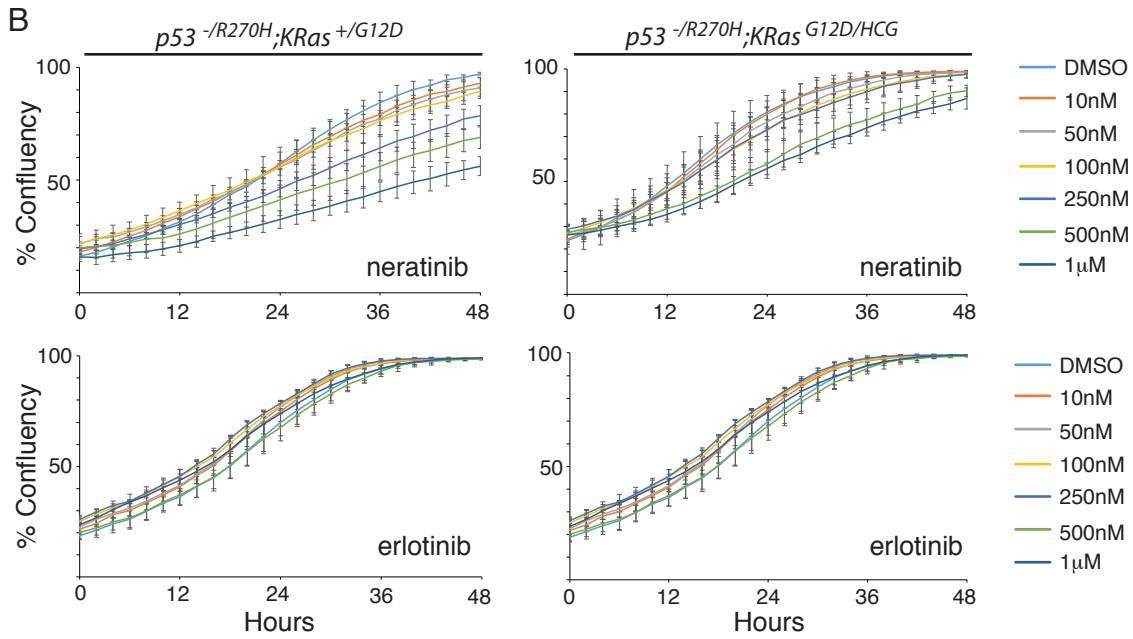
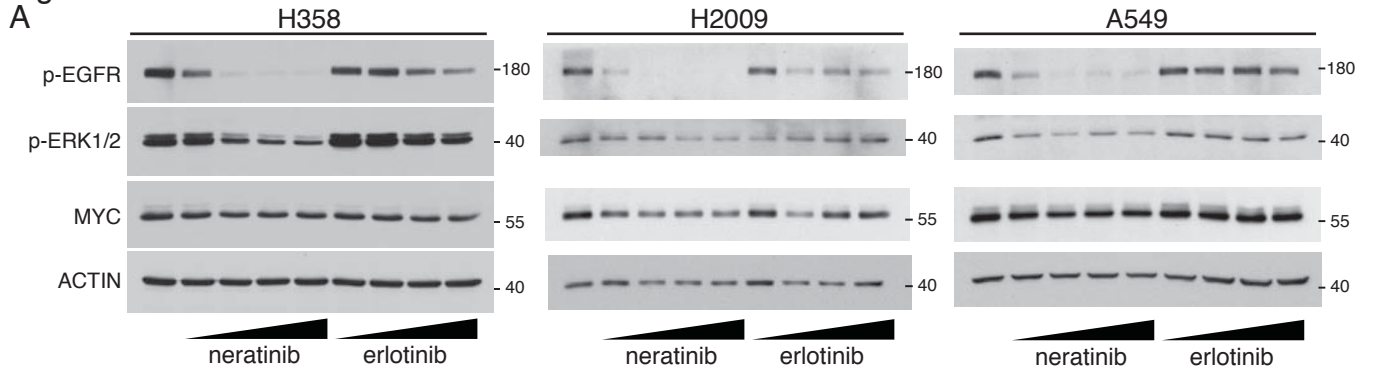
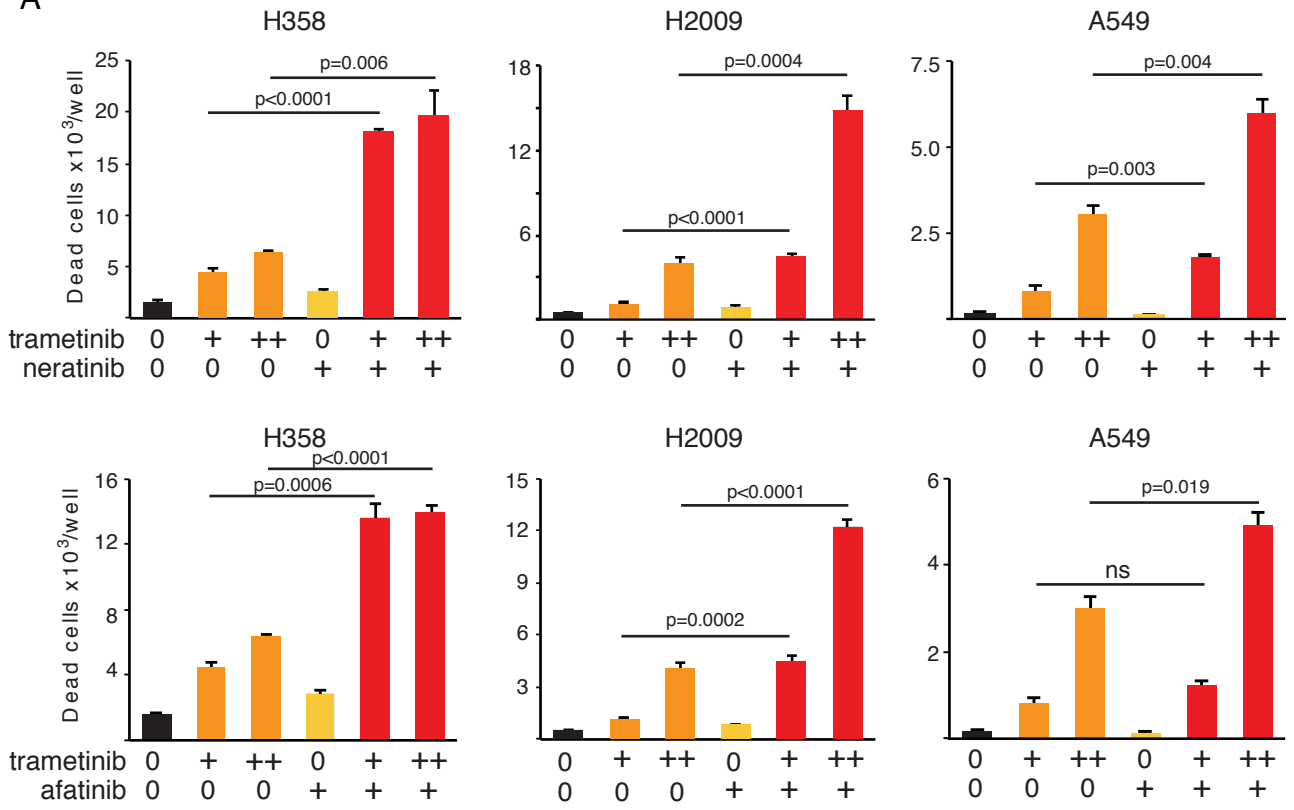


Figure S4: Sensitivity of KRAS mutant cell lines to ERBB blockade.

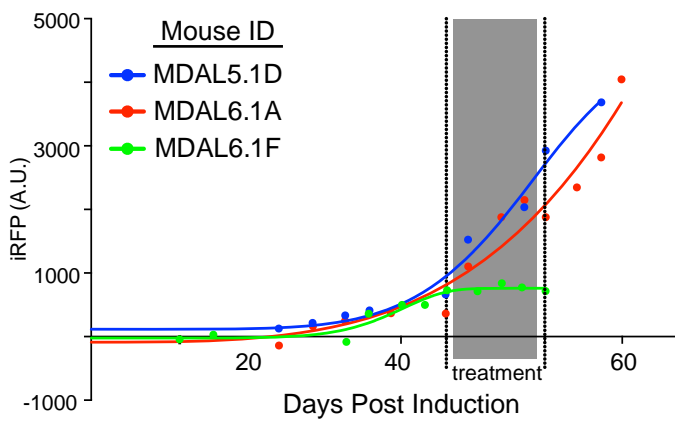
A) Lysates from KRAS-mutant NSCLC cells treated with increasing doses (10, 100, 500 and 1000 nM) of erlotinib or neratinib were subject to immunoblotting with the indicated antibodies. **B)** Growth curves of *Kras*^{G12D/wt};*p53*^{R270H/-} (single copy *KRAS*^{G12D}) and *Kras*^{G12D/HCG};*p53*^{R270H/-} [high copy gain (HCG) *KRAS*^{G12D}] murine lung tumor cell lines treated with the indicated doses of neratinib (upper panels) or erlotinib (lower panels), monitored by Incucyte time lapse video-microscopy. Error bars denote SD of technical triplicates. **C)** Growth curves of RAS-less MEFs reconstituted with wt (left panel) or G12D mutant (center panel) *KRAS* and treated with the indicated doses of neratinib. Error bars indicate SEM of biological triplicates. Right panel shows p-ERK and p-AKT immunoblots of lysates from *KRAS*^{G12D}-expressing MEFs treated with or without neratinib. **D)** RAF-RBD binding assay in RAS-less MEFs reconstituted with *KRAS* G12D, treated with 1 μM neratinib (nera) or vehicle control (vc), immunoblotted with pan-RAS or *KRAS*-specific antibodies. The right panel shows quantification from 3 independent experiments (T-Test).

Figure S5

A



B



C

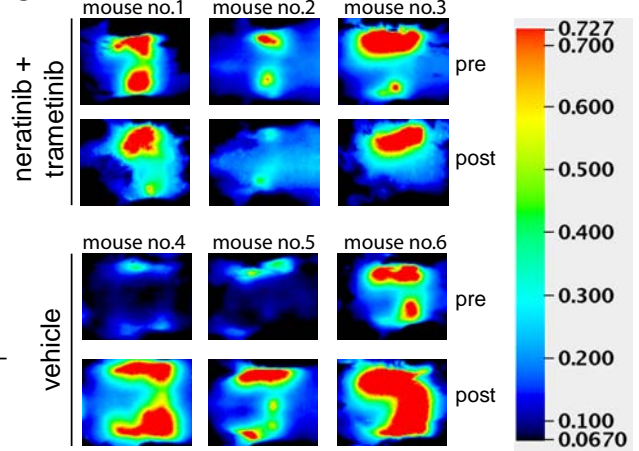


Figure S5: Longitudinal in vivo imaging of nascent lung tumors.

A) Quantification of cell death in KRAS-mutant human lung cancer lines upon treatment with neratinib (250 nM; upper panels) or afatinib (1 μ M; lower panels), alone or in combination with 2 doses (10 nM or 100 nM) of the MEK inhibitor trametinib. Mean and SEM values from a representative experiment are shown. ns = not significant. Lower doses of drugs were used for H358 cells (50 nM afatinib or neratinib and 10 or 50 nM trametinib) due to their greater sensitivity to each drug alone. **B)** KM mice were interbred with *Hprt-lsl-iRFP*, induced with adeno-CRE as before, and monitored for tumor growth using a Licor PEARL imager. Circles indicate days of imaging. Data are normalized to background fluorescence for each mouse, set to 0, and signal intensity curves were calculated using the Weibull growth equation (Graphpad Prism). Upon consistent detection of pulmonary fluorescence, MDAL6-1F was treated with the combination of neratinib + trametinib, while MDAL5.1D and MDAL6.1A received vehicle control for 1 week (gray bar). The presence of tumors was confirmed upon sacrifice. **C)** Representative images of mice treated as per (B) showing fluorescent detection of iRFP-labeled KM tumors before and after drug (or vehicle) treatment. The same colorimetric scale was used for each image. Images are cropped to show only the chest area.

Table S1

Modulated during progression to p-ERK + tumors			Modulated by neratinib in vitro					
Pathway	Rank	FDR	H358		H2009		A549	
			Rank	FDR	Rank	FDR	Rank	FDR
Cytoskeletal remodeling, TGF, WNT pathways	1	1.70E-24	1	2.70E-26	1	1.50E-26	1	2.30E-27
Cytoskeletal remodeling	2	9.00E-23	2	3.20E-21	2	2.10E-22	4	2.40E-22
Transport - Clathrin-coated vesicle cycle	3	3.60E-19	3	2.50E-18	3	2.20E-21	2	1.40E-22
Apoptosis & survival, NGF/TrkA PI3K signaling	4	1.40E-15	4	4.40E-17	4	7.80E-19	3	1.60E-22
Transcription, Sin3 & NuRD regulated	5	1.60E-15	8	4.90E-16	6	4.10E-17	6	4.90E-18
Immune Response, IL4 signaling	6	9.10E-15	19	2.60E-13	14	6.60E-15	8	7.10E-17
Cell Cycle, influence of Ras & Rho in G1/S	7	2.70E-14	11	7.80E-15	8	5.20E-16	7	5.80E-17
Cell Adhesion, Chemokines & adhesion	8	2.80E-14	7	2.30E-16	17	1.50E-14	19	1.10E-13
Development, TGF-beta receptor signaling	10	2.30E-13	6	2.10E-16	5	1.20E-17	13	1.20E-14
Translation, regulation of EIF4F activity	11	3.20E-13	14	1.10E-13	13	6.60E-15	14	1.20E-14
Development, EGFR signaling	12	4.40E-13	12	1.90E-14	10	6.70E-16	11	4.30E-15
Receptor mediated axon growth repulsion	13	5.40E-13	26	3.00E-12	21	3.00E-13	10	3.40E-15
Androgen receptor activation	14	5.60E-13	5	7.60E-17	16	1.10E-14	15	1.20E-14
Epigenetic regulation of gene expression	16	1.60E-12	21	5.60E-13	22	3.40E-13	16	5.00E-14
IGF family signaling in colorectal cancer	17	1.60E-12	22	5.60E-13	18	3.20E-14	29	2.20E-12
TGFb-dependent induction of EMT via MAPK	18	1.60E-12	31	7.60E-12	25	7.40E-13	26	1.60E-12
NGF/TrkA MAPK-mediated signaling	19	2.10E-12	9	1.30E-15	9	6.70E-16	9	9.00E-16
Regulation of STK3/4 (Hippo) and YAP/TAZ	20	2.90E-12	18	2.60E-13	15	1.10E-14	12	9.40E-15

Table S1: Summary of Metacore GeneGO pathway analysis.

The blue shaded region demarcates pathways modulated as KM tumors progress to pERK^{High} expression, ranked by false discovery rate (FDR). The beige shaded region indicates the rank and FDR of the same pathways upon treatment of the indicated KRAS-mutant human NSCLC cell lines with neratinib.